

Article

# Cloning, Characterization and Expression of the Phenylalanine Ammonia-Lyase Gene (*PaPAL*) from Spruce *Picea asperata*

Yufeng Liu, Lijuan Liu, Shuai Yang, Qian Zeng, Zhiran He and Yinggao Liu \*

College of Forestry, Sichuan Agricultural University, No. 211, Huimin Road, Wenjiang District, Chengdu 611130, China

\* Correspondence: 11468@sicau.edu.cn; Tel.: +86-139-0816-9498

Received: 30 May 2019; Accepted: 22 July 2019; Published: 24 July 2019



**Abstract:** Phenylalanine ammonia-lyase (PAL) is the crucial enzyme of the phenylpropanoid pathway, which plays an important role in plant disease resistance. To understand the function of PAL in *Picea asperata*, in this study, the full-length cDNA sequence of the PAL gene from this species was isolated and named *PaPAL*. The gene contains a 2160-bp open reading frame (ORF) encoding 720 amino acids with a calculated molecular weight of 78.7 kDa and a theoretical isoelectric point of 5.88. The deduced PaPAL protein possesses the specific signature motif (GTITASGDLVPLSYIA) of phenylalanine ammonia-lyases. Multiple alignment analysis revealed that PaPAL has high identity with other plant PALs. The tertiary structure of PaPAL was predicted using PcPAL from *Petroselinum crispum* as a template, and the results suggested that PaPAL may have a similar function to that of PcPAL. Furthermore, phylogenetic analysis indicated that PaPAL has a close relationship with other PALs from the Pinaceae species. The optimal expression condition of recombinant PaPAL in *Escherichia coli* BL21 (DE3) was 0.2 mM IPTG (isopropyl  $\beta$ -D-thiogalactoside) at 16 °C for 4 h, and the molecular weight of recombinant PaPAL was found to be approximately 82 kDa. Recombinant PaPAL was purified and exhibited high PAL activity at optimal conditions of pH 8.6 and 60 °C. Quantitative real-time PCR (qRT-PCR) showed the *PaPAL* gene to be expressed in all tissues of *P. asperata* tested, with the highest expression level in the needles. The *PaPAL* gene was induced by the pathogen (*Lophodermium piceae*), which caused needle cast disease, indicating that it might be involved in defense against needle cast disease. These results provide a basis for understanding the molecular mechanisms of the PAL gene in the process of *P. asperata* disease resistance.

**Keywords:** *Picea asperata*; phenylalanine ammonia-lyase (PAL); molecular cloning; expression

## 1. Introduction

To adapt to changes in the ecological environment and related biotic and abiotic stresses, conifers have evolved a diverse defense system as one of their main strategies for survival [1]. The conifer defense system synthesizes a variety of secondary metabolites when attacked by pathogens, mainly a variety of phenolic compounds, including highly polymerized physical barriers such as lignin, which prevent the invasion of pathogens [2]. These phenolic defense compounds are primarily synthesized by the phenylpropanoid pathway, an important secondary metabolic pathway that produces various key molecules required for the plant defense system and systemic resistance [3–5]. For example, phytoalexins are compounds with antimicrobial activity biosynthesized by the phenylpropanoid pathway that inhibit infectious disease when plants are attacked by pathogens [6,7]. Rosmarinic acid is synthesized from the precursor molecules L-phenylalanine and L-tyrosine, which may play a role in plant defense against fungal and bacterial infections [8]. Salicylic acid is produced by a branch of the

phenylpropanoid pathway and plays an important role in the local and systemic induction of plant resistance to pathogens [9–11]. Lignin functions as a physical barrier reducing damage to the plant cell wall by cell wall-degrading enzymes produced by invading pathogens [2,12–14]. In mango plants, a large number of secondary metabolites are produced by induction of the phenylpropanoid pathway in stem tissue, which increases resistance to *Ceratocystis fimbriata* [15]. In addition, induction of key enzymes in the phenylpropanoid pathway, including phenylalanine ammonia-lyase, enhances the defense of chickpea plants against ascochyta blight disease [16].

Phenylalanine ammonia-lyase (PAL, EC 4.3.1.5), the first and key enzyme in the phenylpropanoid pathway, catalyzes the conversion of phenylalanine to *trans*-cinnamic acid and ammonia by non-oxidative deamination [17,18], which is the key regulatory point of the connection between primary metabolism and secondary metabolism in plants [19]. Due to the importance of PAL in the phenylpropanoid pathway, it has always been a hot research topic [20]. PAL is present in all higher plants studied, and it has also been found in some fungi [21,22], cyanobacteria [23] and *Streptomyces maritimus* [24]. Nevertheless, PAL has not yet been found in eubacteria, archaea or animals [19,25]. PAL genes have been cloned and studied from a variety of plants, such as *Ginkgo biloba* [26], *Lycoris radiata* [27], sugarcane [28] and buckwheat [29]. The relationship between PAL and plant disease resistance is also a focus of research. In tomato plants, expression of PAL genes is positively induced by *Verticillium dahliae* [30]. *OsPAL4* is associated with resistance to bacterial blight, sheath blight, and rice blast in rice [31]. Silencing of *CaPAL1* in pepper plants attenuates resistance to *Xanthomonas campestris* pv. *vesicatoria*, and overexpression of *CaPAL1* in Arabidopsis increases resistance to *Pseudomonas syringae* pv. *tomato* and *Hyaloperonospora arabidopsidis* [11]. Moreover, overexpression of *GmPAL2.1* in transgenic soybean plants enhances resistance to *Phytophthora sojae* [25]. In addition, knockout of four PAL genes in Arabidopsis resulted in susceptibility to *Pseudomonas syringae* [32]. Therefore, the PAL gene is believed to play a positive role in plant disease resistance.

*Picea asperata* from the Pinaceae family, the major afforestation tree in the subalpine forests of southwestern China, is very important in the conservation of water sources and soil as well as in water conservation and regional ecological balance. In recent years, many *P. asperata* plantations have suffered from needle cast disease, and the molecular mechanism of disease resistance is still unclear. In view of the important role of PAL in plant disease resistance, it is necessary to perform research on the role of this gene in the prevention of needle cast disease in *P. asperata*. However, to our knowledge, there is no report on the study of PAL from *P. asperata*; additionally, in *Picea*, the PAL gene has only been reported in Norway spruce [33,34]. Therefore, to understand the function of PAL in *P. asperata* and further explore the relationship between the PAL gene and needle cast disease resistance, we cloned the full-length cDNA of the PAL gene from *P. asperata* and characterized the molecular features, phylogenetic evolution and enzyme activity properties of the recombinant PAL protein. Furthermore, we analyzed the expression profiles of PAL in different tissues and during pathogen infection.

## 2. Materials and Methods

### 2.1. Plant Materials

*P. asperata* (approximately twenty years old) was grown under natural field conditions on a forest farm of Erlang Mountain in Sichuan, China. Roots, phloem, young needles, young fruits and seeds were collected from healthy *P. asperata*. In addition, young needles were collected from healthy *P. asperata* and *P. asperata* infected by the pathogen (*Lophodermium piceae*, its information is shown in Figure S1 of Supplementary Material) causing needle cast disease in May (preinfection), July (early stage of infection), September (middle stage of infection) and November (late stage of infection). The details of the *P. asperata* collection are shown in Supplementary Material Table S1. All samples were immediately frozen in liquid nitrogen and stored at  $-80^{\circ}\text{C}$  for RNA isolation.

## 2.2. RNA Isolation and cDNA Synthesis

Total RNA was isolated from all samples using a Quick RNA Isolation Kit (Huayueyang Biotech Co., Ltd., Beijing, China) following the manufacturer's instructions. The RNA was incubated with RNase-free DNaseI (TaKaRa Bio Inc, Dalian, China) to eliminate genomic DNA. The quality and concentration of the RNA was determined by 1% (M/V) agarose gel electrophoresis and using a BioMate 3S UV-visible spectrophotometer (Thermo, Waltham, MA, USA). First-strand cDNA was synthesized with a PrimeScript™ RT Reagent Kit (TaKaRa Bio Inc, Dalian, China) according to the manufacturer's instructions. The cDNA was stored at −20 °C for cDNA cloning and quantitative real-time PCR (qRT-PCR) analysis.

## 2.3. Cloning of the Full-Length PaPAL cDNA

A pair of specific primers (PaPAL-F1: 5'-GAGGAGTTCAGGACAGG-3' and PaPAL-R1: 5'-TCAGAATGGACCAGGCGTT-3') was designed using Primer Premier Version 5.0 software (PREMIER Biosoft International, Palo Alto, CA, USA) according to the nucleotide sequence of *PAL* from *Picea sitchensis* (GenBank: EF085404.1). The full-length cDNA was amplified in a 25-μL PCR reaction with 1 μL cDNA, 12.5 μL Trans Taq® High Fidelity (HiFi) PCR SuperMix (2 ×) (TransGen Biotech Co., Ltd., Beijing, China), 1 μL each of 10 μM PaPAL-F1 and PaPAL-R1 primers, and 9.5 μL ddH<sub>2</sub>O. The reaction conditions were as follows: Pre-denaturing at 94 °C for 4 min; followed by 35 cycles of 94 °C for 40 s, 57 °C for 40 s, and 72 °C for 2 min 40 s; and a final extension at 72 °C for 10 min. The PCR product was assessed by 1% (M/V) agarose gel electrophoresis and the target fragment was purified with a TIANgel Midi Purification Kit (Tiangen Biotech Co., Ltd., Beijing, China). The purified products were cloned into the pMD19-T vector (TaKaRa Bio Inc, Dalian, China) and then transformed into competent cells of *Escherichia coli* DH5α. The transformed bacteria were screened by blue/white screening and identified by PCR. Positive colonies were sequenced by Shanghai Majorbio Bio-Pharm Technology Co., Ltd. (Shanghai, China).

## 2.4. Bioinformatics Analysis of PaPAL

The open reading frame (ORF) was identified by the ORF Finder tool (<https://www.ncbi.nlm.nih.gov/orffinder/>). The amino acid sequence of *PaPAL* was deduced using DNAMAN Version 6.0 software (Lynnon, Pointe-Claire, QC, Canada). The fundamental physiochemical properties of the protein were predicted by the online tool ProtParam (<https://web.expasy.org/protparam/>). Analysis of sequence homology was carried out by Blast (<https://blast.ncbi.nlm.nih.gov/Blast.cgi>). Multiple sequence alignments were produced with ClustalW version 1.83 [35]. Conserved domains in the protein were detected using the NCBI (National Center for Biotechnology Information) server (<https://www.ncbi.nlm.nih.gov/Structure/cdd/wrpsb.cgi>). Modification sites and conserved residues of the protein were found by PROSITE (Database of protein domains, families and functional sites) (<https://prosite.expasy.org/prosite.html>) and InterPro (<http://www.ebi.ac.uk/interpro/>), respectively. The secondary structure of the protein was predicted by SOPMA (Self-Optimized Prediction Method with Alignment) (<https://npsa-prabi.ibcp.fr>). Predictions of signal peptide and transmembrane regions in the protein were performed with SignalP-5.0 Server (<http://www.cbs.dtu.dk/services/SignalP/>) and TMHMM Server v. 2.0 (<http://www.cbs.dtu.dk/services/TMHMM/>), respectively. Homology modelling was carried out by SWISS-MODEL (<https://swissmodel.expasy.org/>). A phylogenetic tree was constructed based on the neighbor-joining (NJ) method in MEGA version 6.0 [36].

## 2.5. Expression and Purification of PaPAL in *E. coli*

The coding sequence of *PaPAL* was amplified using the primers PaPAL-F2 (5'-GGACTAGT ATGGTTGCAGCTGCAGC-3', the *SpeI* restriction site is underlined) and PaPAL-R2 (5'-CCGCTCGAG TCAGAATGGACCAGGCG-3', the *XhoI* restriction site is underlined). The PCR products were digested with *SpeI* and *XhoI* and then inserted into the pET28a (+) expression vector (TaKaRa Bio Inc, Dalian,

China). The positive recombinant plasmid (named pET28a (+)-*PaPAL*) was verified by sequencing and transformed into the *E. coli* BL21(DE3) strain. A transformant containing pET28a(+)-*PaPAL* was collected and grown in 3 mL of Luria Bertani (LB) culture medium with 50 µg/mL kanamycin at 37 °C until the OD600 (optical density) reached 0.6–0.8. Protein expression was then induced by the addition of 0.6 mM (final concentration) isopropyl β-D-thiogalactoside (IPTG, Merck) at 37 °C. To obtain optimal expression conditions of *PaPAL* in *E. coli*, various temperatures (16, 25, 30 and 37 °C), concentrations of IPTG (0, 0.2, 0.4, 0.6, 0.8 and 1.0 mM), and durations of induction (0, 2, 4, 6, 8 and 10 h) were tested. The protein expression level was assessed by 12% sodium dodecyl sulfate polyacrylamide gel electrophoresis (SDS-PAGE) and visualized by Coomassie Brilliant Blue R-250 staining. After optimal induction, cells were collected by centrifugation and lysed by sonication. The recombinant protein was purified using a His-tag Protein Purification Kit (Beyotime Biotechnol Co., Ltd., Shanghai, China). The purity of the purified protein was analyzed by 12% SDS-PAGE, and its concentration was detected by the Coomassie Brilliant Blue G-250 method.

### 2.6. Enzyme Activity Assay for Recombinant *PaPAL*

The enzyme activity of recombinant *PaPAL* was assayed according to a previous method, with slight modification [37]. The reaction mixture contained 2 mL of 100 mM borate buffer (pH 8.6), 1 mL of 10 mM L-phenylalanine and 100 µL of purified protein; ddH<sub>2</sub>O replaced the protein in the negative control reaction. The reaction mixture was incubated at 40 °C for 30 min and stopped by incubation on ice. Activity was monitored by measuring the formation of trans-cinnamic acid by increased absorbance at 290 nm in a spectrophotometer (BioMate 3S UV-visible, Thermo, Waltham, MA, USA). One unit (U) of enzyme activity was defined as the amount of PAL that catalyzed the formation of 1 µmol of trans-cinnamic acid from L-phenylalanine per minute. To determine the optimal pH, the reaction mixtures were assayed at 40 °C in various borate-buffered solutions (pH 8.0, 8.2, 8.4, 8.6, 8.8 and 9.0). To determine the optimal temperature, reactions were carried out with the optimal pH at varying temperatures (30, 40, 50, 60, 70 and 80 °C).

### 2.7. Expression Properties of *PaPAL* by qRT-PCR

The transcript levels of *PaPAL* in different tissues of *P. asperata* and in young needles from the healthy *P. asperata* and infected *P. asperata* collected at various time points during pathogen infection were analyzed by qRT-PCR using a CFX96™ Real-Time System (Bio-Rad, Hercules, CA, USA). Amplification primers (*PaPAL*-F3: 5'-AAGCAGATTGTTTCTCAAGTAGCCA-3' and *PaPAL*-R3: 5'-GCAGGGATCGTCGATGTAGGA-3', the amplification product is 141 bp) were designed based on the coding sequence of *PaPAL*. The elongation factor-1 alpha gene (GenBank: AJ132534.1, the primers EF-F: 5'-AACTGGAGAAGGAACCCAAG-3' and EF-R: 5'-AACGACCCAATGGAGGATAC-3', the amplification product is 114 bp) [38] and translation initiation factor 5A gene (GenBank: DR448953, the primers TIF5A-F: 5'-GGTCTTCCCTCATCAA-3' and TIF5A-R: 5'-GAGGATGGTTTTGTTAGCC-3', the amplification product is 118 bp) [39] were used as two internal references. qRT-PCR was performed in a 25-µL reaction volume containing 2 µL of 10-fold diluted cDNA, 12.5 µL of TB Green™ Premix Ex Taq™ II (TaKaRa Bio Inc, Dalian, China), 1 µL of (10 µM) forward primer, 1 µL of (10 µM) reverse primer and 8.5 µL ddH<sub>2</sub>O. The reaction conditions were as follows: 1 cycle of 95 °C for 30 s, followed by 40 cycles of 95 °C for 5 s and 60 °C for 30 s, with a final melt curve analysis performed from 65–95 °C. ddH<sub>2</sub>O instead of cDNA was used as a negative control. The tissue with the lowest expression level was selected as the control and assigned a nominal value of 1.0; healthy needles at different stages of infection were selected as the control for the expression characteristics assays. The expression results were analyzed using the comparative cycle threshold (Ct) method and quantified relative to the control ( $2^{-\Delta\Delta C_t}$ ) [37,40].

The qRT-PCR assays were performed in three independent replicates. The data analysis was carried out using SPSS version 20.0 (SPSS Inc., Chicago, IL, USA). The significance of differences was assessed by Duncan's multiple range test ( $p \leq 0.05$ ) and the T test ( $p \leq 0.05$ ). Data are presented as the mean  $\pm$  standard error (SE).

### 3. Results

#### 3.1. Cloning and Characterization of the PaPAL Gene

Using specific primers (PaPAL-F1 and PaPAL-R1), the full-length cDNA sequence of *PAL* was amplified from cDNA of *P. asperata* young needles by RT-PCR. The product was found to be 2303 bp in size (Figure 1) and was designated *PaPAL* (GenBank accession No. MK770350).

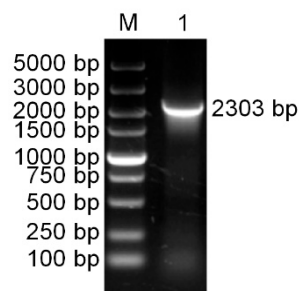


**Figure 1.** The PCR amplification product of the *PaPAL* gene. M: DNA molecular weight standards; 1: The PCR product of full-length cDNA.

The *PaPAL* gene contains a 140-bp 5'-untranslated region and a 2160-bp open reading frame (ORF) encoding 720 amino acids (Figure S2). ProtParam analysis showed that the deduced PaPAL protein has a calculated molecular weight of 78.7 kDa and a theoretical isoelectric point of 5.88. Blast and multiple alignment analysis by ClustalW revealed that PaPAL has high identity with other reported plant PALs in GenBank, sharing 99.44% identity with PsPAL from *Picea sitchensis* (ABK24709.1), 94.44% identity with LkPAL from *Larix kaempferi* (AHA44840.1), and 84.97% identity with GbPAL from *Ginkgo biloba* (ABU49842.1) (Figure 2). NCBI analysis showed that PaPAL contains a phenylalanine ammonia-lyase conserved domain at position 24–720 that belongs to the phenylalanine ammonia-lyase superfamily. Many sites essential for PAL activities were identified by PROSITE and InterPro in PaPAL (Figure S2 and Figure 2). For example, the phenylalanine and histidine ammonia-lyase signature sequence (GTITASGDLVPLSYIA) is present at positions 204–219, containing a key active site motif, Ala-Ser-Gly (208–210), for 3,5-dihydro-5-methylidene-4H-imidazol-4-one (MIO) group formation [41]. In addition, strictly conserved amino acid residues are present in the PaPAL protein, such as Y116, G117, V118, T120, F122, Q137, L140, P257, K258, E259, G260, L261, N265, Y356, R359, N389 and H401. Conserved deamination sites (L213, V214, L261 and A262) and conserved catalytic active sites (N265, G266, NDN387-389, H401 and HNQDV491-495) were also found in PaPAL. Furthermore, PROSITE analysis showed that PaPAL contains 16 N-myristoylation sites, 13 casein kinase II phosphorylation sites, 8 protein kinase C phosphorylation sites, 4 N-glycosylation sites and 1 tyrosine kinase phosphorylation site.

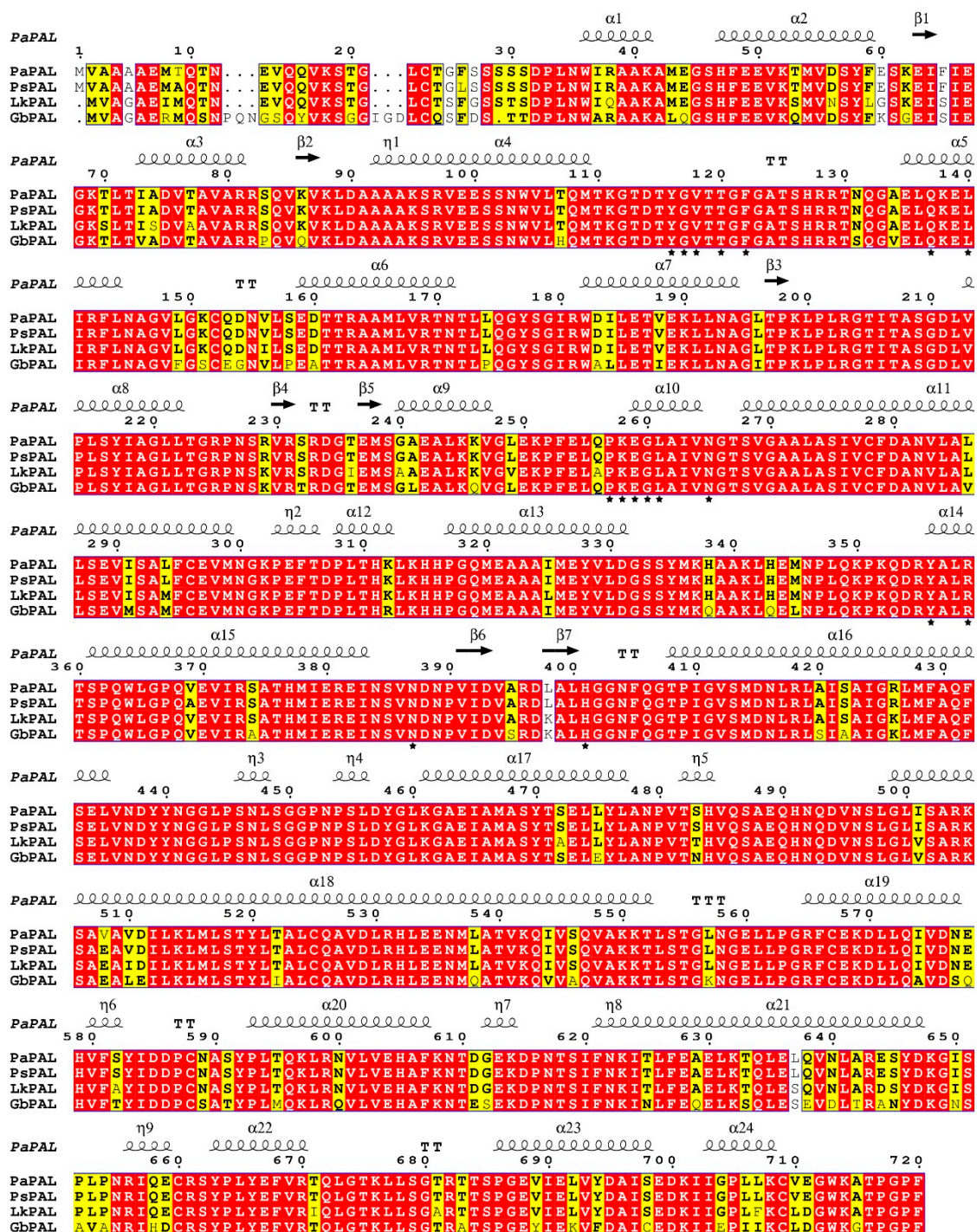


**Figure 2.** Multiple alignment of the deduced PaPAL protein with other plant phenylalanine ammonia-lyase (PAL) proteins. The sequences are from *Picea sitchensis* (PsPAL, ABK24709.1), *Larix kaempferi* (LkPAL, AHA44840.1) and *Ginkgo biloba* (GbPAL, ABU49842.1). Completely identical amino acid sequences are indicated with white words and red backgrounds. Highly conserved amino acid sequences are represented with black words and yellow backgrounds. Non-conserved amino acid sequences are shown with grey words and white backgrounds.  $\alpha$ -Helices are displayed as large squiggles and  $\eta$ -helices as small squiggles. Strict  $\beta$ -turns are shown with TT letters and  $\beta$ -strands as arrows. Strictly conserved amino acid residues are shown as ★.

### 3.2. Analysis of Secondary Structure and Tertiary Structure of the PaPAL Protein

The secondary structure of the PaPAL protein was predicted by the SOPMA tool. The results indicated that PaPAL consists mainly of  $\alpha$ -helices (57.64%) and random coils (29.44%) as well as a few extended strands (7.08%) and beta turns (5.83%) (Figure 3a). To better understand the structure and function of the PaPAL protein, the tertiary structure was predicted using SWISS-MODEL based on the crystal structure of *Petroselinum crispum* PAL (PDB: 1W27) [42]. The model covered the amino acids 31–720 of PaPAL, and its secondary structure is shown in Figure 2. In particular, the tertiary structure of PaPAL consists of four subunits that assume a seahorse shape (Figure 3b) [41]. In addition, each subunit is composed of an MIO domain, a core domain and an inserted shielding domain. The highly conserved Ala-Ser-Gly triad, which acts as an active site for cyclization and dehydration for MIO group formation, was also found within the MIO domain [5].

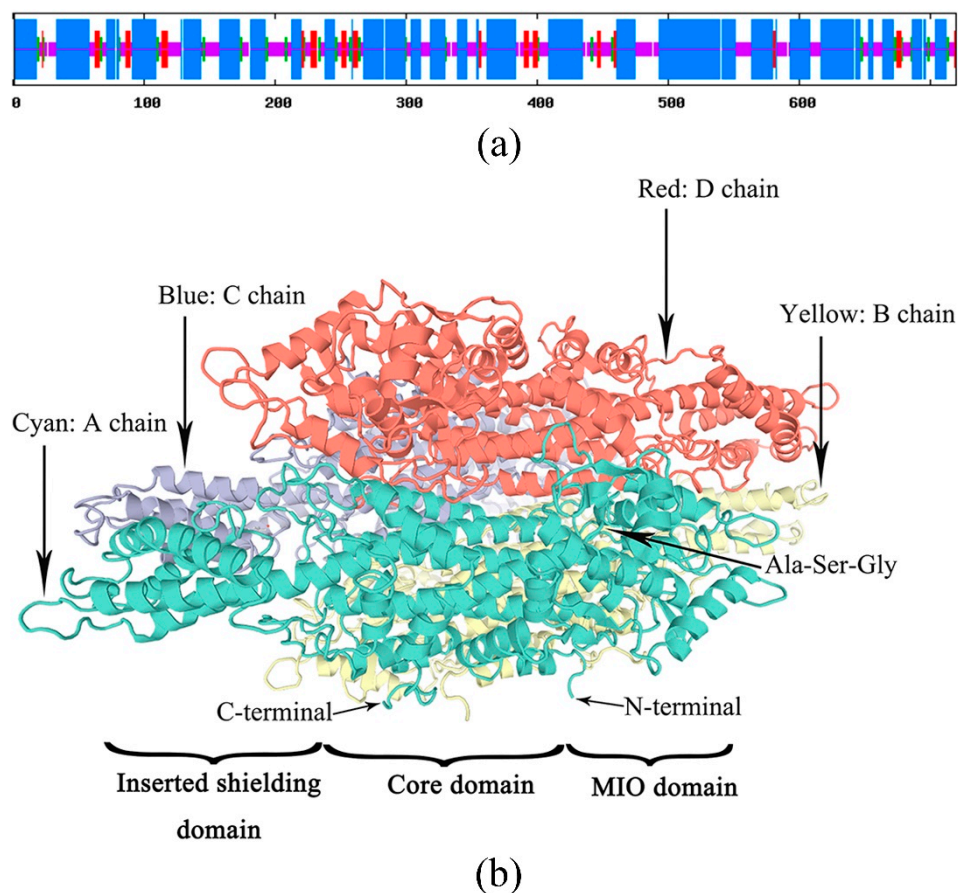


**Figure 3.** Prediction of PaPAL structure. (a) Prediction of PaPAL secondary structure;  $\alpha$ -helix, random coil, extended strand and beta turn are represented with blue, pink, red and green regions, respectively. (b) Prediction of PaPAL tertiary structure.

### 3.3. Phylogenetic Analysis of PaPAL

To explore the evolutionary relationship between PaPAL and PALs from other plants, MEGA 6.0 was used to construct a phylogenetic tree by the neighbor-joining method. As shown in Figure 4, the phylogenetic tree was in good agreement with the traditional taxonomy classification, with grouping into four main clusters, similar to those reported by Zhu et al. [37] and Wu et al. [4]. These four main clusters include angiosperm, gymnosperm, bryophyta and pteridophyta. Moreover, the dicotyledon and monocotyledon species independently formed each of the subfamilies in the angiosperm family. Interestingly, four lianas from different families in dicotyledon were clustered together. The PALs from Rosaceae species and those from Pinaceae species were clustered together. The result grouped PaPAL

with other PALs from Pinaceae species; a close relationship to PsPAL from *Picea sitchensis* was also indicated. Comprehensively, the results suggested that PaPAL might have a common evolutionary ancestor with other PALs and a similar function in the phenylpropanoid pathway.

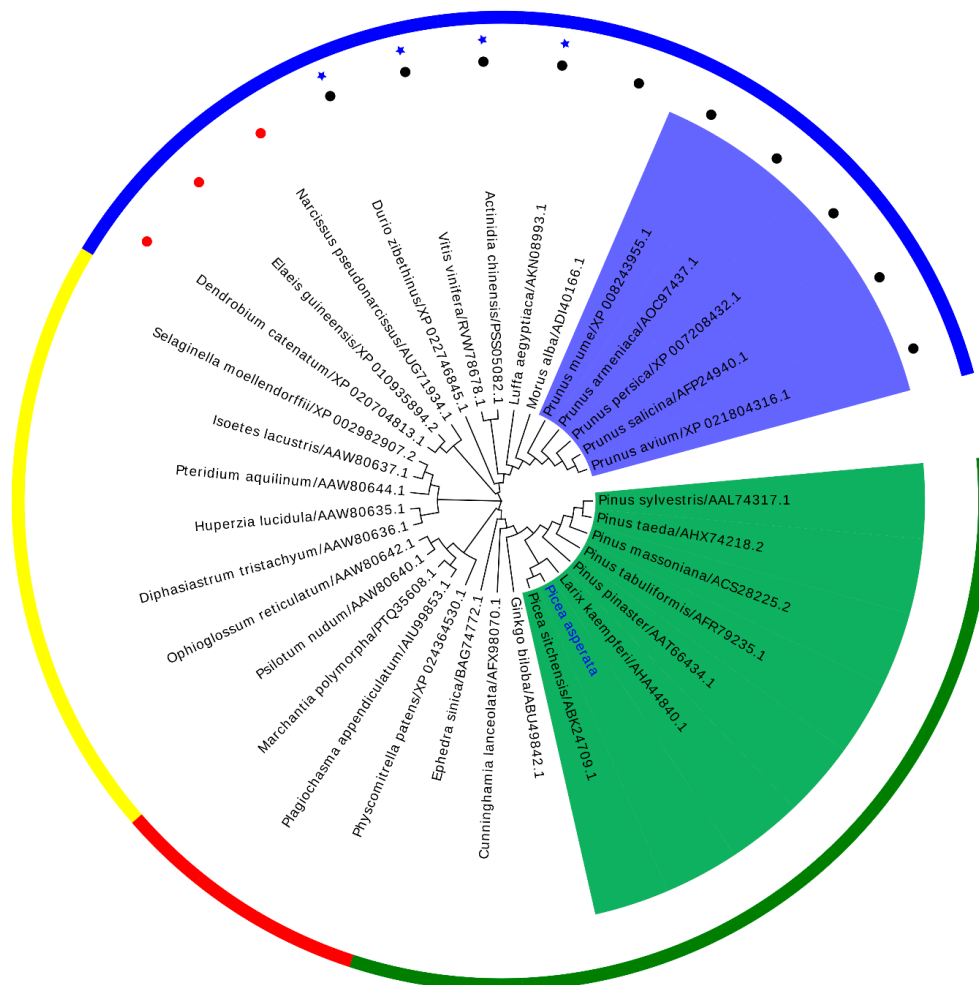


**Figure 4.** A phylogenetic tree between PaPAL and other plant PALs was constructed by the neighbor-joining (NJ) method. Outer circle: Gymnosperm species are shown in green, bryophyta species in red, pteridophyta species in yellow, angiosperm species in blue. The liana species are represented in ★. The monocot species and dicotyledon species are represented with ● and ●, respectively. Inner ring: Rosaceae species are indicated with a blue background and Pinaceae species with a green background.

### 3.4. Expression, Purification and Functional Characterization of Recombinant PaPAL

To confirm PaPAL protein expression in *E. coli* and determine its functional activities, a recombinant plasmid was constructed using the pET28a (+) vector. In addition, induction expression conditions were optimized to obtain the maximum amount of PaPAL protein. According to SDS-PAGE analysis, the molecular weight of recombinant PaPAL was approximately 82 kDa, which was consistent with the expected size of PaPAL (approximately 79 kDa) fused to a 3 kDa His-tag peptide (Figure 5a). Moreover, the recombinant PaPAL protein was not detected in the negative controls (including empty-vector pET28a(+) in *E. coli* BL21(DE3) with 0.6 mM IPTG added, empty-vector pET28a(+) in *E. coli* BL21(DE3) with no IPTG added and pET28a(+)-PaPAL in *E. coli* BL21(DE3) with no IPTG added). The highest expression level of recombinant PaPAL was detected by adding 0.2 mM IPTG (Figure 5a) followed by incubation for 4 h (Figure 5b). Furthermore, the distribution of recombinant PaPAL in the supernatant and precipitate was detected (Figure 5c). Most of recombinant PaPAL was found in

inclusion bodies, and the proportion in the soluble fraction increased slightly with decreasing induction temperature. Therefore, recombinant PaPAL was produced with induction of 0.2 mM IPTG at 16 °C for 4 h. Recombinant PaPAL was purified by 6×His-tag affinity (Figure 5d), and the concentration of the purified protein was 0.83 mg/mL.

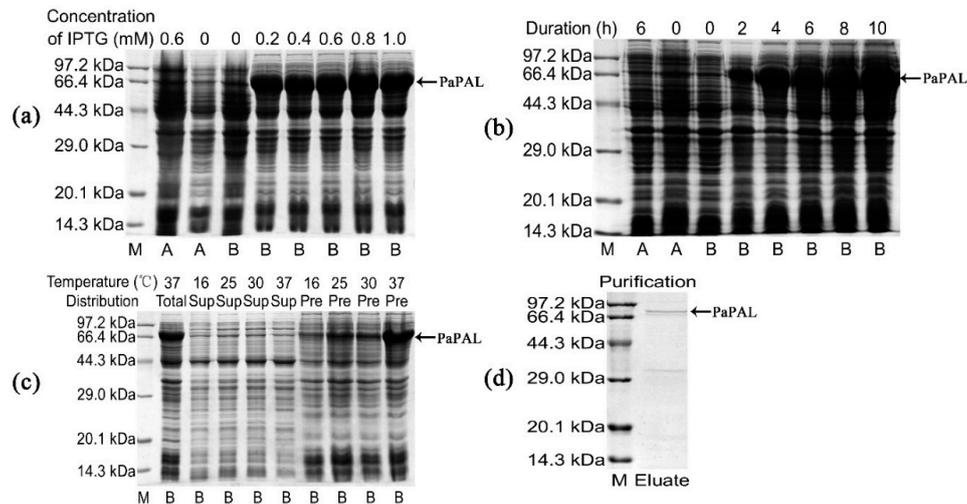


**Figure 5.** Sodium dodecyl sulfate polyacrylamide gel electrophoresis (SDS-PAGE) analysis of recombinant PaPAL expression and purification. M: Protein molecular mass marker; A: pET28a(+) in *E. coli* BL21(DE3); B: pET28a(+)-PaPAL in *E. coli* BL21(DE3); negative controls: pET28a(+) in *E. coli* BL21(DE3) with 0.6 mM IPTG added, pET28a(+) in *E. coli* BL21(DE3) with no IPTG added and pET28a(+)-PaPAL in *E. coli* BL21(DE3) with no IPTG added; (a) pET28a(+)-PaPAL in *E. coli* BL21(DE3) was induced with different concentrations of IPTG (0.2–1.0 mM) at 37 °C for 6 h; (b) pET28a(+)-PaPAL in *E. coli* BL21(DE3) was induced with 0.2 mM IPTG for 0, 2, 4, 6, 8 and 10 h at 37 °C; (c) pET28a(+)-PaPAL in *E. coli* BL21(DE3) was induced with 0.2 mM IPTG for 4 h at different temperatures (16 °C, 25 °C, 30 °C and 37 °C), and the total protein, supernatant and precipitate of cell lysate were analyzed; (d) purified recombinant PaPAL.

A high level of PAL activity was determined for the purified recombinant PaPAL protein. The optimal pH was 8.6, with activity for converting *L*-phenylalanine to trans-cinnamic acid of 3224.10 U/mg at this pH (Figure 6a). In addition, the optimal temperature of recombinant PaPAL activity was determined to be 60 °C, and its catalytic activity was 4536.14 U/mg at this temperature (Figure 6b).

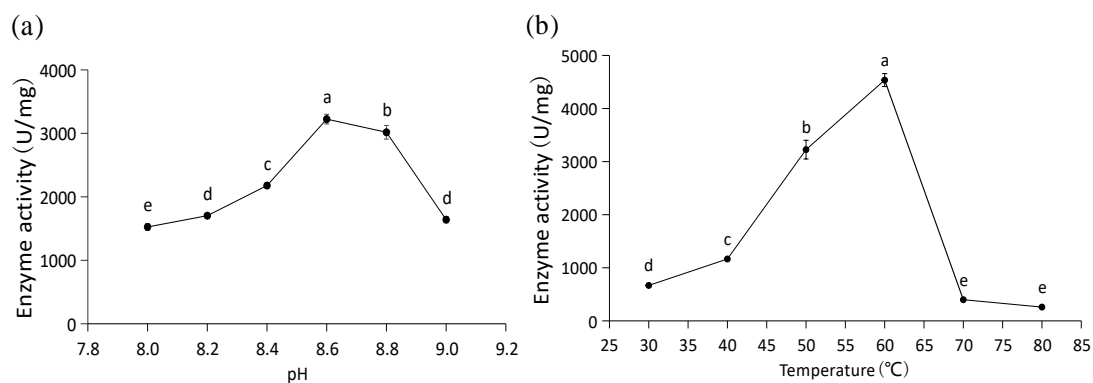


**Figure 6.** Functional characterization of recombinant PaPAL. (a) Optimal pH analysis of recombinant PaPAL; (b) optimal temperature analysis of recombinant PaPAL. The data represent the mean values of three replicates  $\pm$  standard errors (SEs). The different letters (a, b, c, d and e) on the SE line represent statistically significant differences at  $p \leq 0.05$  (Duncan's multiple range test).

### 3.5. Transcriptional Profiles of PaPAL in Different Tissues and at Different Periods during Pathogen Infection

The expression levels of PaPAL in *P. asperata* were analyzed by qRT-PCR. PaPAL transcripts were detected in all of the tissues examined (Figure 7a). The lowest expression level was found in the seed, which was normalized to 1. The highest expression level was determined in needles, followed young fruit. The expression levels of PaPAL in the root and phloem were similar.

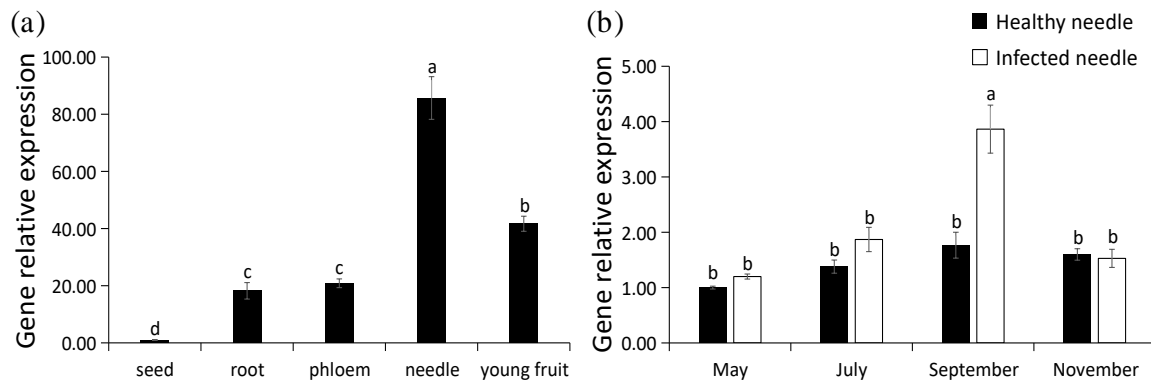


**Figure 7.** Transcription pattern of PaPAL. (a) Relative expression level of PaPAL in different tissues of *P. asperata*; (b) relative expression level of PaPAL at different periods during pathogen infection. The data represent the mean values of three replicates  $\pm$  standard errors (SEs). The different letters (a, b, c and d) on the SE line represent statistically significant differences at  $p \leq 0.05$  (Duncan's multiple range test and T test, respectively).

With the increase of infection time of needle cast disease during the year, proportion of needles infected by *Lophodermium piceae* gradually increased, and September was the most serious period of needle infection (Table S1). To evaluate PaPAL expression is induced by biotic stress, transcript levels of PaPAL in *P. asperata* were examined during infection by the pathogen (*Lophodermium piceae*) causing needle cast disease. As shown in Figure 7b, there was no difference in the expression levels of PaPAL gene between healthy *P. asperata* and infected *P. asperata* in May (preinfection). However, PaPAL transcript accumulation in infected *P. asperata* increased to 1.36-fold of that in the healthy *P. asperata* in July (the early stage of infection). By September (the middle stage of infection), PaPAL transcript accumulation in infected *P. asperata* increased significantly and reached the highest level (2.19-fold of that in the healthy *P. asperata*). Subsequently, the PaPAL expression levels in both healthy *P. asperata* and infected *P. asperata* decreased in November (the late stage of infection).

## 4. Discussion

PAL-mediated catalysis is the rate-limiting step of the phenylpropanoid pathway, which controls the biosynthesis of secondary metabolites in plants, such as lignins, flavonoids and phytoalexins, in plants [3,27,43,44]. These compounds play an important role in plant resistance to pathogen infection and insect attack [9,45–47]. In this study, the full-length cDNA sequence of PaPAL from *P. asperata* was isolated and analyzed. The coding sequence of PaPAL is 2160 bp in size, which is larger than *SmpALs* (2127–2133 bp) from *Salvia miltiorrhiza* [48], *RgPAL* (2121 bp) from *Rhodotorula glutinis* [49], and *BoPAL1* (2139 bp) from *Bambusa oldhamii* [50] and smaller than *PtPAL* (2265 bp) from *Pinus taeda* [1] and *FtPAL* (2166 bp) from *Fagopyrum tataricum* [44], and encodes 720 amino acids. Multiple alignment analysis showed that the PaPAL protein sequence has high similarity with that of other reported PAL proteins, indicating that the PAL protein has been highly conserved during evolution. The conserved motif (GTITASGDLVPLSYIA), which is a specific signature sequence of phenylalanine ammonia-lyase [41,51], was detected at positions 204–219 of the PaPAL protein. In addition, the active site sequence (Ala-Ser-Gly), which is considered to be key for the formation of the MIO group [52], is present in the conserved motif of PaPAL. Conserved deamination sites (L213, V214, L261 and A262) and catalytic

active sites (N265, G266, NDN387-389, H401 and HNQDV491-495) are thought to play an important role in the function of the PAL protein [3,19,53]. These sites were also found in the PaPAL protein, suggesting that PaPAL has a similar function to that of other PALs. PaPAL contains five types of modification sites, i.e., N-myristoylation, casein kinase II phosphorylation, protein kinase C phosphorylation, N-glycosylation and tyrosine kinase phosphorylation sites, which are also reported for ObPAL [54]. The first tertiary structure of PAL was determined for that from *Rhodospiridium toruloides* [55], and the first crystal structure was characterized for that from *Petroselinum crispum* [41]. *Petroselinum crispum* PAL is a homotetramer, and each subunit assumes a seahorse shape [44]. The tertiary structure of PaPAL was homology modeled using *Petroselinum crispum* PAL as a template, and four 'seahorse shape' subunits were also observed. Thus far, the seahorse shape has been reported for *Melissa officinalis* [56], *Solenostemon scutellarioides* [37] and *Ocimum basilicum* [54]. The results suggest that PaPAL might have catalytic functions similar to those of other PAL proteins. It is well known that monocotyledon and dicotyledon PALs form independent each subfamilies [27,57]. Our phylogenetic tree also agreed well with the genetic evolution of spermatophytes. PaPAL clustered together with other PALs from Pinaceae species, such as *Pinus taeda* [1]. In addition, PaPAL shows the closest relationship with the PAL of *Picea sitchensis*. We also found that lianas clustered together, even though they derived from different families.

In most plants, PAL is encoded by a small family of 2–13 members, such as in *Arabidopsis thaliana* [32,58,59], *Pinus taeda* [1], *Salvia miltiorrhiza* [60], *Bambusa oldhamii* [50] and *Ginkgo biloba* [26]. In this study, only one PAL gene from in *P. asperata* was isolated and characterized. However, as it remains unknown whether a PAL gene family exists in *P. asperata* and how many family members there are, further studies need to be conducted.

A heterologous protein of interest can be obtained by expressing a target gene in a prokaryote such as *E. coli*, facilitating the study of the functional and enzymatic properties of the target protein [61]. The prokaryotic expression system has the advantages of high yield, easy operation, good stability and low cost [62,63], providing an effective approach for examining the expression and functional characteristics of the PaPAL protein. The recombinant PaPAL protein was successfully expressed in *E. coli* using a prokaryotic expression vector, pET-28a(+), and its molecular weight was found to be approximately 82 kDa by SDS-PAGE analysis. To obtain a large amount of PaPAL, expression was optimized by testing different induction conditions. In general, high-level expression of recombinant protein in *E. coli* results in the formation of inclusion bodies [64]. As expected, the recombinant PaPAL protein was also found mainly in inclusion bodies. Higher culture temperature increases the rate of recombinant protein synthesis and the concentration of polymeric intermediates, thereby promoting the formation of inclusion bodies [65], whereas soluble proteins is promoted by a lower culture temperature [66]. When expression of recombinant PaPAL was induced at 16 °C, we found that the amount of soluble protein increased slightly in the supernatant. ObPAL from *Ocimum basilicum* was expressed in *E. coli* using the pET-28a(+) vector, and the result showed that the content of recombinant protein was also low [54]. In contrast, the content of recombinant RcPAL was increased in the supernatant, also expressed in *E. coli* using the pET-28a(+) vector [67]. We suspect that the cause of the difference in expression might be because the genes are from different species. The expression level of soluble protein may be improved by assessing other effective expression vectors and expression conditions. Other plant PALs have also been successfully expressed in vitro, such as those from *Jatropha curcas* [52], *Fagopyrum tataricum* [44] and *Solenostemon scutellarioides* [37].

To demonstrate the function of the PaPAL protein, recombinant PaPAL was purified using a Ni<sup>2+</sup>-agarose column, and the purified protein was obtained at a concentration of 0.83 mg/mL. When L-phenylalanine was used as the substrate, the purified PaPAL protein exhibited high PAL activity, as expected. In addition, the characteristics of PaPAL were further analyzed. The optimal pH of recombinant PaPAL was 8.6, similar to that of PAL from *Oryza sativa* (8.5) [68] and within the range known for plant PALs [49,69]. The enzyme activity of recombinant PaPAL was determined to be 3224.10 U/mg at pH 8.6. Moreover, the optimal temperature of recombinant PaPAL was 60 °C, which was

the same as that of PALs from *Salvia miltiorrhiza* [60], *Jatropha curcas* [52], *Solenostemon scutellarioides* [37] and *Ocimum basilicum* [54] and close to that of PALs from *Petroselinum crispum* (58 °C) [70] and *Zea mays* (55–60 °C) [71] but higher than that of PALs from *Bambusa oldhamii* (50 °C) [50], *Rhus chinensis* (45 °C) [67] and *Arabidopsis thaliana* (31–48 °C) [69]. The enzyme activity of recombinant PaPAL at 60 °C was determined to be 4536.14 U/mg.

To date, tissue expression of the *PAL* genes has been studied in a variety of plants [60,72–75]. In our study, the highest expression level was observed in the needles of *P. Asperata*, and the lowest in the seeds. High expression levels of the *PAL* gene in leaves have been found in *Petroselinum crispum* [76], *Rehmannia glutinosa* [75], *Isatis indigotica* [77], *Salvia miltiorrhiza* [60] and *Solenostemon scutellarioides* [37]. In addition, it has been reported that the transcription levels of *GbPAL* in *Ginkgo biloba* correlated significantly with flavonoid accumulation, and the *GbPAL* gene was also highly expressed in leaves [26]. Therefore, high expression in needles may suggest a high rate of flavonoid biosynthesis in *P. asperata*. *PAL* genes were also occasionally highly expressed in the roots of *Nicotiana tabacum* [78], *Rubus idaeus* [74] and *Astragalus membranaceus* [79], which may be due to the high rate of lignification for root development [5]. Moreover, a high expression level of the *PAL* gene in stems [44,67] and flowers [52] has been reported.

Many studies have shown that expression of the *PAL* gene can be induced by pathogens [4,80]. In this study, qRT-PCR analysis revealed that *PaPAL* gene expression was upregulated during infection of the needle cast disease pathogen *Lophodermium piceae* infection, which suggested that the *PaPAL* gene is involved in the *P. asperata* defense response. With the gradual aggravation of needle cast disease during this year, expression of the *PaPAL* gene in infected plants showed a pattern of increasing first and then decreasing. The result was similar to the expression pattern of the *HbPAL* gene from the white root rot disease-tolerant rubber clone PB5/51 during *Rigidoporus microporus* infection [3]. In addition, a number of studies have found that the *PAL* gene exhibits a rapid response in the early stages of pathogen infection [4]. However, expression of the *PAL* gene in flax showed a pattern of continuous increase during pathogen infection [81]. In brief, the *PaPAL* gene can be induced by *Lophodermium piceae*, and we speculated that PaPAL plays an active role in the defense against needle cast disease.

## 5. Conclusions

In this study, we successfully isolated and characterized the *P. asperata PaPAL* gene, which contains the specific signature sequence and active site of phenylalanine ammonia-lyases. Bioinformatics analysis showed that PaPAL has high sequence identity and structural similarity with other reported plant PAL proteins. Furthermore, we successfully expressed and purified the PaPAL protein in vitro, which exhibited high PAL enzyme activity. qRT-PCR analysis revealed that the highest expression level of the *PaPAL* gene occurs in needles of *P. asperata*. In particular, our study demonstrates that the *PaPAL* gene is involved in the response to needle cast disease pathogen (*Lophodermium piceae*) infection. This work provides fundamental information for understanding the role of the *PaPAL* gene in *P. asperata* and lays the foundation for further exploration of the function of *P. asperata PaPAL* in defense against needle cast disease.

**Supplementary Materials:** The following are available online at <http://www.mdpi.com/1999-4907/10/8/613/s1>, Figure S1: The information of pathogen (*Lophodermium piceae*). (a) The ascoma of *L. piceae* on the needle of *Picea asperata*; (b) The transverse section of *L. piceae* ascoma; (c) The ascospore of *L. piceae*; (d) The conidium of *L. piceae*. *L. piceae* characteristic sequence Genbank ID: KX573897, Table S1: The details of the *Picea asperata* collection conditions on a forest farm of Erlang Mountain in Sichuan, China, Figure S2: Nucleotide sequence and the deduced amino acid sequence of the *PaPAL* gene. The start codon and stop codon are indicated by bold font and an asterisk, respectively. The phenylalanine and histidine ammonia-lyase signature sequence is underlined. The deamination sites are shaded in grey. The catalytic active sites are shown in boxes.

**Author Contributions:** Conceptualization, Y.L. (Yufeng Liu); methodology, Y.L. (Yufeng Liu) and Y.L. (Yinggao Liu); validation, Y.L. (Yufeng Liu), L.L., S.Y., Q.Z., Z.H. and Y.L. (Yinggao Liu); formal analysis, Y.L. (Yufeng Liu); investigation, S.Y., Q.Z. and Z.H.; resources, Y.L. (Yinggao Liu); data curation, Y.L. (Yufeng Liu) and Y.L. (Yinggao Liu); writing—original draft preparation, Y.L. (Yufeng Liu); writing—review and editing, Y.L. (Yufeng Liu) and Y.L. (Yinggao Liu); visualization, L.L. and Z.H.; supervision, Y.L. (Yinggao Liu); project administration, Y.L. (Yufeng Liu).

**Funding:** This research received no external funding.

**Acknowledgments:** We would like to thank Y.L. (Yufeng Liu) and Y.L. (Yinggao Liu) for the conception and design of the experiments, Y.L. (Yufeng Liu), L.L., S.Y. and Z.H. for carrying out the experiments, Y.L. (Yufeng Liu) and Q.Z. for their contributions to the discussion and analysis of the experiments., We would also like to thank Y.L. (Yinggao Liu) for providing experimental materials, Y.L. (Yufeng Liu) for writing the paper.

**Conflicts of Interest:** The authors declare no conflicts of interests.

## References

1. Bagal, U.R.; Leebens-Mack, J.H.; Lorenz, W.W.; Dean, J.F. The phenylalanine ammonia lyase (PAL) gene family shows a gymnosperm-specific lineage. *BMC Genom.* **2012**, *13*, S1.
2. Bonello, P.; Gordon, T.R.; Herms, D.A.; Wood, D.L.; Erbilgin, N. Nature and ecological implications of pathogen-induced systemic resistance in conifers: A novel hypothesis. *Physiol. Mol. Plant Pathol.* **2006**, *68*, 95–104.
3. Sangsil, P.; Nualsri, C.; Woraathasin, N.; Nakkanong, K. Characterization of the phenylalanine ammonia lyase gene from the rubber tree (*Hevea brasiliensis* Müll. Arg.) and differential response during *Rigidoporus microporus* infection. *J. Plant Prot. Res.* **2016**, *56*, 380–388.
4. Wu, Z.H.; Gui, S.T.; Wang, S.Z.; Ding, Y. Molecular evolution and functional characterisation of an ancient phenylalanine ammonia-lyase gene (*NnPAL1*) from *Nelumbo nucifera*: Novel insight into the evolution of the PAL family in angiosperms. *BMC Evol. Biol.* **2014**, *14*, 100.
5. Xu, F.; Deng, G.; Cheng, S.Y.; Zhang, W.Y.; Huang, X.H.; Li, L.L.; Cheng, H.; Rong, X.F.; Li, J.B. Molecular cloning, characterization and expression of the phenylalanine ammonia-lyase gene from *Juglans regia*. *Molecules* **2012**, *17*, 7810–7823. [[PubMed](#)]
6. Bowles, D.J. Defense-related proteins in higher plants. *Annu. Rev. Biochem.* **1990**, *59*, 873–907. [[PubMed](#)]
7. Cho, M.H.; Lee, S.W. Phenolic phytoalexins in rice: Biological functions and biosynthesis. *Int. J. Mol. Sci.* **2015**, *16*, 29120–29133.
8. Petersen, M.; Abdullah, Y.; Benner, J.; Eberle, D.; Gehlen, K.; Hücherig, S.; Janiak, V.; Kim, K.H.; Sander, M.; Weitzel, C.; et al. Evolution of rosmarinic acid biosynthesis. *Phytochemistry* **2009**, *70*, 1663–1679.
9. Clarke, J.D.; Volko, S.M.; Ledford, H.; Ausubel, F.M.; Dong, X. Roles of salicylic acid, jasmonic acid, and ethylene in cpr-induced resistance in arabidopsis. *Plant Cell* **2000**, *12*, 2175–2190.
10. Suzuki, H.; Xia, Y.; Cameron, R.; Shadle, G.; Blount, J.; Lamb, C.; Dixon, R.A. Signals for local and systemic responses of plants to pathogen attack. *J. Exp. Bot.* **2004**, *55*, 169–179.
11. Kim, D.S.; Hwang, B.K. An important role of the pepper phenylalanine ammonia-lyase gene (*PAL1*) in salicylic acid-dependent signalling of the defense response to microbial pathogens. *J. Exp. Bot.* **2014**, *65*, 2295–2306. [[PubMed](#)]
12. Iiyama, K.; Lam, T.B.; Stone, B.A. Covalent cross-links in the cell wall. *Plant Physiol.* **1994**, *104*, 315–320. [[PubMed](#)]
13. Bhuiyan, N.H.; Selvaraj, G.; Wei, Y.; King, J. Role of lignification in plant defense. *Plant Signal. Behav.* **2009**, *4*, 158–159. [[PubMed](#)]
14. Collinge, D.B. Cell wall appositions: The first line of defense. *J. Exp. Bot.* **2009**, *60*, 351–352. [[PubMed](#)]
15. Araujo, L.; Bispo, W.M.S.; Rios, V.S.; Fernandes, S.A.; Rodrigues, F.A. Induction of the phenylpropanoid pathway by acibenzolar-s-methyl and potassium phosphite increases mango resistance to *Ceratocystis fimbriata* infection. *Plant Dis.* **2015**, *99*, 447–459. [[PubMed](#)]
16. Kavousi, H.R.; Marashi, H.; Bagheri, A.R.; Mozafari, J. Expression of phenylpropanoid pathway genes in chickpea defense against race 3 of ascochyta rabiei. *Plant Pathol. J.* **2009**, *8*, 127–132.
17. Yusuf, C.Y.L.; Abdullah, J.O.; Shaharuddin, N.A.; Abu Seman, I.; Abdullah, M.P. Characterization of promoter of *EgPAL1*, a novel PAL gene from the oil palm *Elaeis guineensis* Jacq. *Plant Cell Rep.* **2018**, *37*, 265–278.
18. Koukol, J.; Conn, E.E. The metabolism of aromatic compounds in higher plants. IV. Purification and properties of the phenylalanine deaminase of *Hordeum vulgare*. *J. Biol. Chem.* **1961**, *236*, 2692–2698.
19. Jin, Q.; Yao, Y.; Cai, Y.P.; Lin, Y. Molecular cloning and sequence analysis of a phenylalanine ammonia-lyase gene from *Dendrobium*. *PLoS ONE* **2013**, *8*, e62352.
20. Jiang, Y.M.; Xia, B.; Liang, L.J.; Li, X.D.; Xu, S.; Peng, F.; Wang, R. Molecular and analysis of a phenylalanine ammonia-lyase gene (*LrPAL2*) from *Lycoris radiata*. *Mol. Biol. Rep.* **2013**, *40*, 2293–2300.

21. Kim, S.H.; Kronstad, J.W.; Ellis, B.E. Purification and characterization of phenylalanine ammonia-lyase from *Ustilago maydis*. *Phytochemistry* **1996**, *43*, 351–357.
22. Hattori, T.; Nishiyama, A.; Shimada, M. Induction of l-phenylalanine ammonia-lyase and suppression of veratryl alcohol biosynthesis by exogenously added l-phenylalanine in a white-rot fungus *Phanerochaete chrysosporium*. *FEMS Microbiol. Lett.* **1999**, *179*, 305–309. [[PubMed](#)]
23. Moffitt, M.C.; Louie, G.V.; Bowman, M.E.; Pence, J.; Noel, J.P.; Moore, B.S. Discovery of two cyanobacterial phenylalanine ammonia lyases: Kinetic and structural characterization. *Biochemistry* **2007**, *46*, 1004–1012. [[PubMed](#)]
24. Xiang, L.K.; Moore, B.S. Biochemical characterization of a prokaryotic phenylalanine ammonia lyase. *J. Bacteriol.* **2005**, *187*, 4286–4289. [[PubMed](#)]
25. Zhang, C.Z.; Wang, X.; Zhang, F.; Dong, L.D.; Wu, J.J.; Cheng, Q.; Qi, D.Y.; Yan, X.F.; Jiang, L.Y.; Fan, S.J.; et al. Phenylalanine ammonia-lyase2.1 contributes to the soybean response towards *Phytophthora sojae* infection. *Sci. Rep.* **2017**, *7*, 7142.
26. Xu, F.; Cai, R.; Cheng, S.; Du, H.; Wang, Y. Molecular cloning, characterization and expression of phenylalanine ammonia-lyase gene from *Ginkgo biloba*. *Afr. J. Biotechnol.* **2008**, *7*, 721–729.
27. Jiang, Y.M.; Xia, N.; Li, X.D.; Shen, W.B.; Liang, L.J.; Wang, C.Y.; Wang, R.; Peng, F.; Xia, B. Molecular cloning and characterization of a phenylalanine ammonia-lyase gene (*LrPAL*) from *Lycoris radiata*. *Mol. Biol. Rep.* **2011**, *38*, 1935–1940.
28. Kasirajan, L.; Aruchamy, K.; Thirugnanasambandam, P.P.; Athiappan, S. Molecular cloning, characterization, and expression analysis of lignin genes from Sugarcane genotypes varying in lignin content. *Appl. Biochem. Biotechnol.* **2017**, *181*, 1270–1282. [[PubMed](#)]
29. Thiyagarajan, K.; Vitali, F.; Tolaini, V.; Galeffi, P.; Cantale, C.; Vikram, P.; Singh, S.; De Rossi, P.; Nobili, C.; Procacci, S.; et al. Genomic characterization of phenylalanine ammonia lyase gene in Buckwheat. *PLoS ONE* **2016**, *11*, e151187.
30. Gayoso, C.; Pomar, F.; Novo-Uzal, E.; Merino, F.; Ilárduya, O.M.D. The Ve-mediated resistance response of the tomato to *Verticillium dahliae* involves H<sub>2</sub>O<sub>2</sub>, peroxidase and lignins and drives PAL gene expression. *BMC Plant Biol.* **2010**, *10*, 232.
31. Tonnessen, B.W.; Manosalva, P.; Lang, J.M.; Baraoidan, M.; Bordeos, A.; Mauleon, R.; Oard, J.; Hulbert, S.; Leung, H.; Leach, J.E. Rice phenylalanine ammonia-lyase gene *OsPAL4* is associated with broad spectrum disease resistance. *Plant Mol. Biol.* **2015**, *87*, 273–286. [[PubMed](#)]
32. Huang, J.L.; Gu, M.; Lai, Z.B.; Fan, B.F.; Shi, K.; Zhou, Y.H.; Yu, J.Q.; Chen, Z.X. Functional analysis of the Arabidopsis PAL gene family in plant growth, development, and response to environmental stress. *Plant Physiol.* **2010**, *153*, 1526–1538. [[PubMed](#)]
33. Yaqoob, N.; Yakovlev, I.A.; Krokene, P.; Kvaalen, H.; Solheim, H.; Fossdal, C.G. Defense-related gene expression in bark and sapwood of Norway spruce in response to *Heterobasidion parviporum* and methyl jasmonate. *Physiol. Mol. Plant Pathol.* **2012**, *77*, 10–16.
34. Koutaniemi, S.; Warinowski, T.; Kärkönen, A.; Alatalo, E.; Fossdal, C.G.; Saranpää, P.; Laakso, T.; Fagerstedt, K.V.; Simola, L.K.; Paulin, L.; et al. Expression profiling of the lignin biosynthetic pathway in Norway spruce using EST sequencing and real-time RT-PCR. *Plant Mol. Biol.* **2007**, *65*, 311–328. [[PubMed](#)]
35. Thompson, J.D.; Higgins, D.G.; Gibson, T.J. CLUSTAL W: Improving the sensitivity of progressive multiple sequence alignment through sequence weighting, position-specific gap penalties and weight matrix choice. *Nucleic Acids Res.* **1994**, *22*, 4673–4680. [[PubMed](#)]
36. Tamura, K.; Stecher, G.; Peterson, D.; Filipski, A.; Kumar, S. MEGA6: Molecular evolutionary genetics analysis version 6.0. *Mol. Biol. Evol.* **2013**, *30*, 2725–2729. [[PubMed](#)]
37. Zhu, Q.L.; Xie, X.R.; Lin, H.X.; Sui, S.Z.; Shen, R.X.; Yang, Z.F.; Lu, K.; Li, M.Y.; Liu, Y.G. Isolation and functional characterization of a phenylalanine ammonia-lyase gene (*SsPAL1*) from *Coleus (Solenostemon scutellarioides)* (L.) Codd. *Molecules* **2015**, *20*, 16833–16851. [[PubMed](#)]
38. Zhang, T.; Zhang, D.; Liu, Y.J.; Luo, C.B.; Zhou, Y.N.; Zhang, L.Y. Overexpression of a NF-YB3 transcription factor from *Picea wilsonii* confers tolerance to salinity and drought stress in transformed *Arabidopsis thaliana*. *Plant Physiol. Biochem.* **2015**, *94*, 153–164. [[PubMed](#)]
39. Kolosova, N.; Breuil, C.; Bohlmann, J. Cloning and characterization of chitinases from interior spruce and lodgepole pine. *Phytochemistry* **2014**, *101*, 32–39. [[PubMed](#)]

40. Livak, K.J.; Schmittgen, T.D. Analysis of relative gene expression data using real-time quantitative PCR and the 2- $\Delta\Delta$ <sup>CT</sup> method. *Methods* **2001**, *25*, 402–408. [[PubMed](#)]
41. Macdonald, M.J.; D’Cunha, G.B. A modern view of phenylalanine ammonia lyase. *Biochem. Cell Biol.* **2007**, *85*, 273–282. [[PubMed](#)]
42. Ritter, H.; Schulz, G.E. Structural basis for the entrance into the phenylpropanoid metabolism catalyzed by phenylalanine ammonia-lyase. *Plant Cell* **2004**, *16*, 3426–3436. [[PubMed](#)]
43. Hahlbrock, K.; Scheel, D. Physiology and molecular biology of phenylpropanoid metabolism. *Annu. Rev. Plant Physiol. Plant Mol. Biol.* **1989**, *40*, 347–369.
44. Li, C.L.; Bai, Y.C.; Chen, H.; Zhao, H.X.; Shao, J.R.; Wu, Q. Cloning, characterization and functional analysis of a phenylalanine ammonia-lyase gene (*FtPAL*) from *Fagopyrum tataricum* Gaertn. *Plant Mol. Biol. Rep.* **2012**, *30*, 1172–1182.
45. Chaman, M.E.; Copaja, S.V.; Argandoña, V.H. Relationships between salicylic acid content, phenylalanine ammonia-lyase (PAL) activity, and resistance of barley to aphid infestation. *J. Agric. Food Chem.* **2003**, *51*, 2227–2231.
46. Harborne, J.B.; Williams, C.A. Advances in flavonoid research since 1992. *Phytochemistry* **2000**, *55*, 481–504. [[PubMed](#)]
47. Li, H.; Yu, Y.; Li, Z.Z.; Arkorful, E.; Yang, Y.Y.; Liu, X.Q.; Li, X.H.; Li, R.L. Benzothiadiazole and b-aminobutyric acid induce resistance to *Ectropis obliqua* in tea plants (*Camellia sinensis* (L.) O. Kuntz). *Molecules* **2018**, *23*, 1290.
48. Hou, X.M.; Shao, F.J.; Ma, Y.M.; Lu, S.F. The phenylalanine ammonia-lyase gene family in *Salvia miltiorrhiza*: Genome-wide characterization, molecular cloning and expression analysis. *Mol. Biol. Rep.* **2013**, *40*, 4301–4310.
49. Zhu, L.B.; Cui, W.J.; Fang, Y.Q.; Liu, Y.; Gao, X.X.; Zhou, Z.M. Cloning, expression and characterization of phenylalanine ammonia-lyase from *Rhodotorula glutinis*. *Biotechnol. Lett.* **2013**, *35*, 751–756.
50. Hsieh, L.S.; Hsieh, Y.L.; Yeh, C.S.; Cheng, C.Y.; Yang, C.C.; Lee, P.D. Molecular characterization of a phenylalanine ammonia-lyase gene (*BoPAL1*) from *Bambusa oldhamii*. *Mol. Biol. Rep.* **2011**, *38*, 283–290.
51. Mahesh, V.; Rakotomalala, J.J.; Le Gal, L.; Vigne, H.; de Kochko, A.; Hamon, S.; Noirot, M.; Campa, C. Isolation and genetic mapping of a *Coffea canephora* phenylalanine ammonia-lyase gene (*CcPAL1*) and its involvement in the accumulation of caffeoyl quinic acids. *Plant Cell Rep.* **2006**, *25*, 986–992. [[PubMed](#)]
52. Gao, J.H.; Zhang, S.W.; Cai, F.; Zheng, X.J.; Lin, N.; Qin, X.B.; Ou, Y.C.; Gu, X.P.; Zhu, X.H.; Xu, Y.; et al. Characterization, and expression profile of a phenylalanine ammonia lyase gene from *Jatropha curcas* L. *Mol. Biol. Rep.* **2012**, *39*, 3443–3452. [[PubMed](#)]
53. Dehghan, S.; Sadeghi, M.; Pöppel, A.; Fischer, R.; Lakes-Harlan, R.; Kavousi, H.R.; Vilcinskis, A.; Rahnamaeian, M. Differential inductions of phenylalanine ammonia-lyase and chalcone synthase during wounding, salicylic acid treatment, and salinity stress in safflower, *Carthamus tinctorius*. *Biosci. Rep.* **2014**, *34*, e114.
54. Khakdan, F.; Alizadeh, H.; Ranjbar, M. Molecular cloning, functional characterization and expression of a drought inducible phenylalanine ammonia-lyase gene (*ObPAL*) from *Ocimum basilicum* L. *Plant Physiol. Biochem.* **2018**, *130*, 464–472. [[PubMed](#)]
55. Calabrese, J.C.; Jordan, D.B.; Boodhoo, A.; Sariaslani, S.; Vannelli, T. Crystal structure of phenylalanine ammonia lyase: Multiple helix dipoles implicated in catalysis. *Biochemistry* **2004**, *43*, 11403–11416.
56. Weitzel, C.; Petersen, M. Enzymes of phenylpropanoid metabolism in the important medicinal plant *Melissa officinalis* L. *Planta* **2010**, *232*, 731–742. [[PubMed](#)]
57. Okada, T.; Mikage, M.; Sekita, S. Molecular characterization of the phenylalanine ammonia-lyase from *Ephedra sinica*. *Biol. Pharm. Bull.* **2008**, *31*, 2194–2199.
58. Wanner, L.A.; Li, G.; Ware, D.; Somssich, I.E.; Davis, K.R. The phenylalanine ammonia-lyase gene family in *Arabidopsis thaliana*. *Plant Mol. Biol.* **1995**, *27*, 327–338.
59. Raes, J.; Rohde, A.; Christensen, J.H.; Van de Peer, Y.; Boerjan, W. Genome-wide characterization of the lignification toolbox in Arabidopsis. *Plant Physiol.* **2003**, *133*, 1051–1071.
60. Song, J.; Wang, Z.Z. Molecular cloning, expression and characterization of a phenylalanine ammonia-lyase gene (*SmPAL1*) from *Salvia miltiorrhiza*. *Mol. Biol. Rep.* **2008**, *36*, 939–952.
61. Bassard, J.E.; Richert, L.; Geerinck, J.; Renault, H.; Duval, F.; Ullmann, P.; Schmitt, M.; Meyer, E.; Mutterer, J.; Boerjan, W. Protein-protein and protein-membrane associations in the lignin pathway. *Plant Cell* **2012**, *24*, 4465–4482. [[PubMed](#)]

62. Esposito, D.; Chatterjee, D.K. Enhancement of soluble protein expression through the use of fusion tags. *Curr. Opin. Biotechnol.* **2006**, *17*, 353–358. [[PubMed](#)]
63. Li, S.J.; Zhang, B.Y.; Zhu, H.M.Y.; Zhu, T.H. Cloning and expression of the chitinase encoded by ChiKJ406136 from *Streptomyces sampsonii* (Millard & Burr) Waksman KJ40 and its antifungal effect. *Forests* **2018**, *9*, 699.
64. Oneda, H.; Inouye, K. Refolding and recovery of recombinant human matrix metalloproteinase 7 (matrilysin) from inclusion bodies expressed by *Escherichia coli*. *J. Biochem.* **1999**, *126*, 905–911. [[PubMed](#)]
65. Baneyx, F. Recombinant protein expression in *Escherichia coli*. *Curr. Opin. Biotechnol.* **1999**, *10*, 411–421. [[PubMed](#)]
66. Urban, A.; Ansmant, I.; Motorin, Y. Optimisation of expression and purification of the recombinant Yol066 (Rib2) protein from *Saccharomyces cerevisiae*. *J. Chromatogr. B* **2003**, *786*, 187–195.
67. Ma, W.L.; Wu, M.; Wu, Y.; Ren, Z.M.; Zhong, Y. Cloning and characterisation of a phenylalanine ammonia-lyase gene from *Rhus chinensis*. *Plant Cell Rep.* **2013**, *32*, 1179–1190.
68. Sarma, A.D.; Sharma, R. Purification and characterization of uv-b induced phenylalanine ammonia-lyase from rice seedlings. *Phytochemistry* **1999**, *50*, 729–737.
69. Cochrane, F.C.; Davin, L.B.; Lewis, N.G. The Arabidopsis phenylalanine ammonia lyase gene family: Kinetic characterization of the four PAL isoforms. *Phytochemistry* **2004**, *65*, 1557–1564.
70. Logemann, E.; Parniske, M.; Hahlbrock, K. Modes of expression and common structural features of the complete phenylalanine ammonia-lyase gene family in parsley. *Proc. Natl. Acad. Sci. USA* **1995**, *92*, 5905–5909.
71. Rösler, J.; Krekel, F.; Amrhein, N.; Schmid, J. Maize phenylalanine ammonia-lyase has tyrosine ammonia-lyase activity. *Plant Physiol.* **1997**, *113*, 175–179. [[PubMed](#)]
72. Dixon, R.A.; Paiva, N.L. Stress-induced phenylpropanoid metabolism. *Plant Cell* **1995**, *7*, 1085–1097. [[PubMed](#)]
73. Zhu, Q.; Dabi, T.; Beeche, A.; Yamamoto, R.; Lawton, M.A.; Lamb, C. Cloning and properties of a rice gene encoding phenylalanine ammonia-lyase. *Plant Mol. Biol.* **1995**, *29*, 535–550. [[PubMed](#)]
74. Kumar, A.; Ellis, B.E. The phenylalanine ammonia-lyase gene family in raspberry. Structure, expression, and evolution. *Plant Physiol.* **2001**, *127*, 230–239. [[PubMed](#)]
75. Lee, B.K.; Park, M.R.; Srinivas, B.; Chun, J.C.; Kwon, I.S.; Chung, I.M.; Yoo, N.H.; Choi, K.G.; Yun, S.J. Induction of phenylalanine ammonia-lyase gene expression by paraquat and stress-related hormones in *Rehmannia glutinosa*. *Mol. Cells* **2003**, *16*, 34–39. [[PubMed](#)]
76. Appert, C.; Logemann, E.; Hahlbrock, K.; Schmid, J.; Amrhein, N. Structural and catalytic properties of the four phenylalanine ammonia-lyase isoenzymes from parsley (*Petroselinum crispum* Nym.). *Eur. J. Biochem.* **1994**, *225*, 491–499. [[PubMed](#)]
77. Lu, B.B.; Du, Z.; Ding, R.X.; Zhang, L.; Yu, X.J.; Liu, C.H.; Chen, W.S. Cloning and characterization of a differentially expressed phenylalanine ammonia-lyase gene (*liPAL*) after genome duplication from tetraploid *Isatis indigotica* Fort. *J. Integr. Plant Biol.* **2006**, *48*, 1439–1449.
78. Pellegrini, L.; Rohfritsch, O.; Fritig, B.; Legrand, M. Phenylalanine ammonia-lyase in tobacco. Molecular cloning and gene expression during the hypersensitive reaction to tobacco mosaic virus and the response to a fungal elicitor. *Plant Physiol.* **1994**, *106*, 877–886.
79. Liu, R.R.; Xu, S.H.; Li, J.L.; Hu, Y.L.; Lin, Z.P. Expression profile of a PAL gene from *Astragalus membranaceus* var. *Mongholicus* and its crucial role in flux into flavonoid biosynthesis. *Plant Cell Rep.* **2006**, *25*, 705–710.
80. Vogt, T. Phenylpropanoid biosynthesis. *Mol. Plant* **2010**, *3*, 2–20.
81. Wojtasik, W.; Kulma, A.; Dymińska, L.; Hanuza, J.; Czemplik, M.; Szopa, J. Evaluation of the significance of cell wall polymers in flax infected with a pathogenic strain of *Fusarium oxysporum*. *BMC Plant Biol.* **2016**, *16*, 75.

